Long glass fiber orientation in thermoplastic composites using a model that accounts for the flexibility of the fibers

Ortman, K.C.[1], G.M. Vélez[2], A.P.R. Eberle[1], D.G. Baird[1] and P. Wapperom[3]

Chemical Engineering Department[1] Virginia Tech, Blacksburg, VA 24061
Macromolecular Science and Engineering Department[2], Virginia Tech, Blacksburg, VA 24061
Mathematics Department[3], Virginia Tech, Blacksburg, VA 24061

Abstract

Mechanical properties of long glass fiber composites, used in various industrial applications, are dependant upon the fiber orientation within the part. To date, however, simulations with the ability to predict fiber orientation as a function of mold design are not available. In this study, several options are explored to predict the orientation of long glass fibers in the concentrated regime that take the flexible nature of these fibers into account. Flow through a center gated disk geometry is simulated numerically for high concentrations of long glass fiber in a polypropylene (PP) matrix. For this, a flow uncoupled 2D finite element (FEM) analysis was performed using a discontinuous Galerkin method for the orientation equations. Numerical results, based on the uncoupled simulations, are compared with experiment for verification.

Introduction

In an effort to produce lightweight energy efficient parts with high moduli, thermoplastics are reinforced with fibers to increase their stiffness, strength, and impact toughness. Such fibers of interest, within this research, are long glass fibers. Currently, glass fiber provides a relatively inexpensive means of producing high strength materials used in energy demanding structures such as automobiles, buildings, and aircraft[9]. Additionally, long glass fibers provide much higher properties, such as Izod Notch Impact (ASTM D256) strength and flexural modulus, in the finished part as compared to the same part manufactured with short glass fibers, and are therefore are the focus of this research. Here the term "long" is used to describe a fiber that may exhibit flexibility in the presence of polymer melt flow, whereas "short" fibers will be said to remain rigid under such deformation.

In order to obtain parts with optimum mechanical properties, it is desired to predict fiber orientation and configuration as a function of mold design and processing conditions. Hence, the goal of this work is to understand the dynamic behavior of long glass fibers in complex polymer melt flow. Much work has been accomplished in simulating the orientation of short glass fibers in polymeric melts[5,7], however relatively few efforts have produced applicable models that can be efficiently used to model long glass fiber orientation. This is, in part, due to the flexible nature of the long glass fibers, whereas short fibers are assumed to be rigid. In this research, we explore several models, in a complex flow, that take the semi-flexible nature of long glass fibers into affect. We then compare these to experimentally determined results.

Experimental Methods

In this research, long fiber orientation is studied in isothermal pressure driven flow between two center gated parallel disks. Forty weight percent, 11 mm long glass fibers, pultruded in a polypropylene matrix, is extruded into the parallel disk geometry with a gap height dimension of approximately 2 mm and a short shot radius of approximately 53 mm (Figure 1).

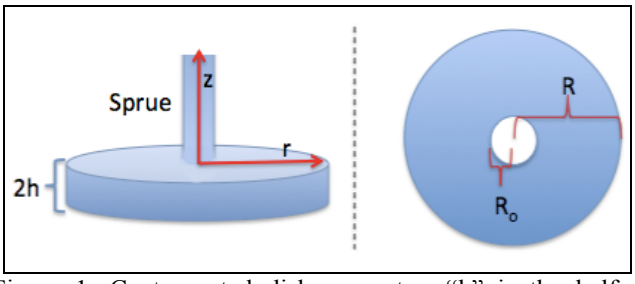

Figure 1: Center gated disk geometry, "h" is the half thickness and "R" and "R_o" are the outside and inside radii of the disk, respectively.

In this research, the flow field is assumed to be uncoupled from the fiber orientation dynamics and can therefore be solved analytically[4] for cylindrical coordinates:

$$v_r(r,z) = \frac{3\dot{Q}}{8\pi h r}\left[1-\left(\frac{z}{h}\right)^2\right] \quad (1)$$

$$v_z(r,z) = 0 \quad (2)$$

In these equations, h is half of the thickness of the disk and $\dot{Q}$ is the volumetric flow rate. The experimental fill time of such a disk is approximately 1 second.

Fiber orientation, within this research, is experimentally measured using the method proposed by Leeds. This method refers to optically analyzing metallographically polished fiber samples, in a plane of

interest. In general, a surface of the injection molded sample may have fibers intersecting it from various angles (Figure 2).

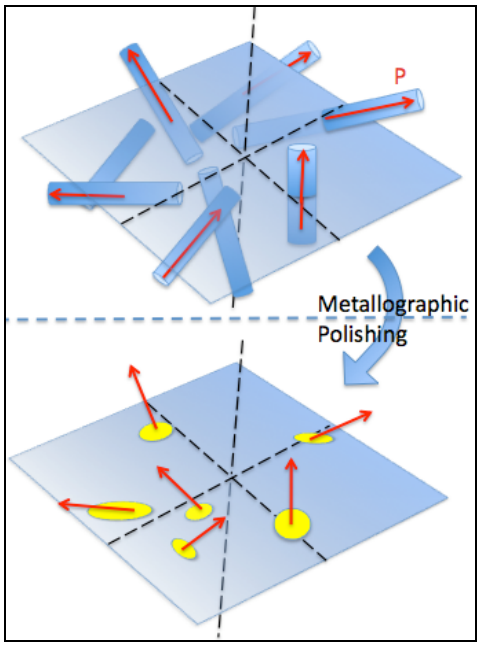

Figure 2: Top: Surface exhibiting fibers with various orientations with respect to the plane. Bottom: Metallographically polished surface exhibiting ellipses.

The angle with which the fiber intersects the plane is determined by its tangential orientation vector. The word "tangential" is used here because a fiber that exhibits flexibility will have curvature. The plane of interest is then metallographically polished to reveal the ellipse with which the fiber penetrated the plane (Figure 2). The sample is then digitally analyzed to recreate the geometry of the ellipses. This information can then be used to determine the vector components of the fiber's orientation[6]. Injection molded samples, in this paper, are analyzed in the "*r-z*" plane at 40% of the short shot length.

Orientation

Fiber orientation may be predicted by an orientation distribution function[2], $\psi(\vec{p})$, where $\vec{p}$ denotes a unit vector that is parallel to the orientation of a rigid fiber (Figure 3). Here, $\psi(\vec{p})$ represents the probability density of finding a fiber with a specific orientation, and thus may be used to determine average orientation properties. Furthermore, the distribution function is normalized such that its integration over all configurational space is unity. Though completely valid, the orientation distribution function is cumbersome to work with and is usually used to construct an orientation tensor. This can be accomplished by taking the second moment of the orientation vector with respect to the distribution function (Eqn. 3).

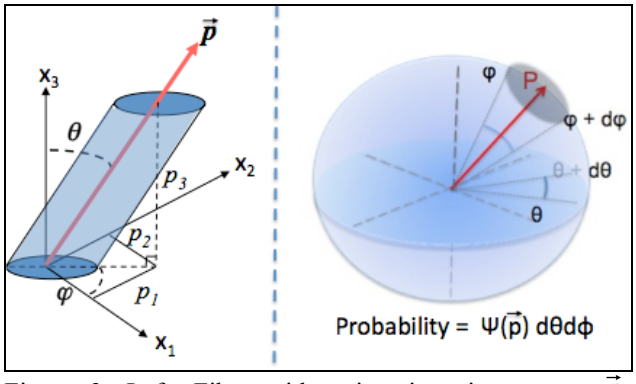

Figure 3: Left: Fiber with unit orientation vector $\vec{p}$. Right: Probability of finding a fiber with the specified orientation.

$$\underline{\underline{A}} = \int \vec{p}\,\vec{p}\,\psi(\vec{p})\,d\vec{p} \qquad (3)$$

$$\underline{\underline{A}}_4 = \int \vec{p}\,\vec{p}\,\vec{p}\,\vec{p}\,\psi(\vec{p})\,d\vec{p} \qquad (4)$$

The orientation tensor provides a measure of the degree of orientation of the fiber in space. Furthermore, the tensor is symmetric and its trace is always equal to unity. Hence, if the A_{11} component is unity ($A_{22} = A_{33} = 0$), then the fiber is fully aligned in the "1" direction (*r* direction for a center gated disk). Furthermore, a fourth order orientation tensor (Eqn. 4) arrives in orientation models as a consequence of the kinematic behavior of the fibers. Numerically, a closure approximation is needed to decouple this tensor into two second order tensors. Although this type of development was formulated for rigid fibers, the models in this research extend the definition of the orientation tensor to flexible fibers by allowing the orientation tensor to describe the tangential orientation of the long fiber.

Models

Now that the tools for quantifying orientation are apparent, a model is needed to explain its dependence within a flow field. Both the Folgar-Tucker[2] model and Bead-Rod model, suggested by Strautins and Latz[7], will be used to try to predict the orientation development of long glass fibers in the specified geometry (Figure 1). The models are used to predict the orientation at 40% of the short shot length starting from an assumed random orientation ($A_{ii} = 1/3$) at the gate (Figure 4). These values are compared experimentally.

Folgar-Tucker Model

The Folgar-Tucker model, which has seen much use since its introduction in the 1980's, was developed for short glass fibers in the concentrated regime. Here, the term concentrated is used to describe the ability for significant fiber-fiber interactions to occur. The model has been developed to extend Jeffry's model, introduced in the early 1920's, by introducing a phenomenological Brownian motion term. This term, called the Folgar-Tucker term, inhibits the steady state alignment of the fibers from being fully oriented.

Generalized Jeffery for Fibers Folgar-Tucker Term

$$\frac{D\underline{\underline{A}}}{Dt} = \left[\underline{\underline{A}} \bullet \underline{\underline{\kappa}}^T + \underline{\underline{\kappa}} \bullet \underline{\underline{A}} - 2\,\underline{\underline{D}} : \underline{\underline{A}}_4 + 2C_I II_D(\underline{\underline{\delta}} - 3\underline{\underline{A}})\right] \quad (5)$$

Within this model, D/Dt is the material derivative, $\underline{\underline{\kappa}}^T$ is the velocity gradient tensor, $\underline{\underline{D}}$ is the rate of strain tensor, C_I is the Folgar-Tucker constant, II_D is the second invariant of the rate of strain tensor, and $\underline{\underline{\delta}}$ is the unit tensor. For the simulation of this model, the quadratic closure approximation is used for the fourth order orientation tensor, within this research.

$$\underline{\underline{A}}_4 = \underline{\underline{A}}\,\underline{\underline{A}} \quad (quadratic\ closure) \qquad (6)$$

Although not discussed here, evaluations of different closure approximations have been reported in the literature[3]. The Folgar-Tucker constant used in this simulation was taken from a previous analysis performed on short glass fibers by Eberle[1], *et al.* whom, through fitting rheological data, determined $C_I = 0.01$. Both fiber evolution models, used in this paper, were accomplished using the discontinuous Galerkin finite element method.

Results for the Folgar-Tucker (FT) model and the experimentally measured data for long glass fiber orientation in the "*r-z*" plane, at 40% of the short shot length, are show in Figure 5.

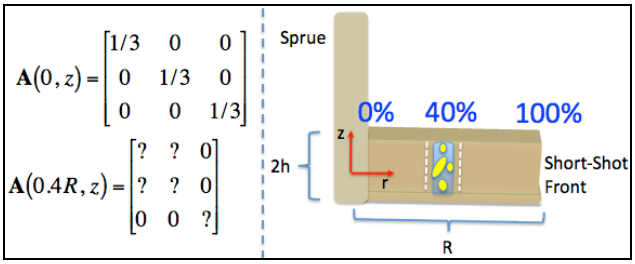

Figure 4: Visual description of mathematical problem using a cylindrical coordinate system. Orientation is assumed random at gate.

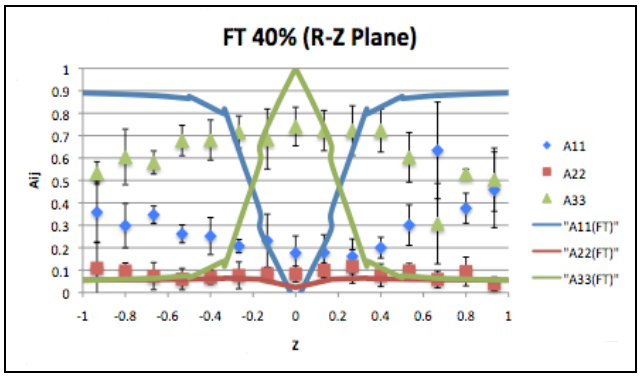

Figure 5: Folgar-Tucker (FT) simulation and experimentally measured results, for the trace components of the orientation tensor, versus the dimensionless mold thickness. The components are give by "r = 1", "z = 2", "θ = 3."

From the experimental data, one will note the relative maxima and minima of the A_{11} and A_{33} components. This behavior is expected to the flow kinematics. The A_{11} component is affected by the shearing flow, which is greater close to the walls of the mold (z = +/- h), where as the A_{33} component is affected by the extensional behavior, which is greater far away from the walls of the mold (z = 0). Hence, the A_{11} components are a maximum near the walls of the mold and pass through a minimum near the center. The opposite is true for the A_{33} component.

Although the Folgar-Tucker model captures this qualitative behavior, the accuracy of it is unsatisfactory (with the exception of A_{22}). The Folgar-Tucker model predicts the location of the maxima and minima correctly, however the values do not agree with experiment. Perhaps most noticeable within Figure 5, Folgar-Tucker model over predicts the rate of change of the A_{11} and A_{33} components. Experimentally it is seen that, although the values pass through local extrema, the rate of change of the components is quite low throughout the height of the part. In our experience, this relatively flat profile seems to be an attribute of long fibers as compared with short fibers.

Bead-Rod Model

The model being referred to here was published in 2007, by Strautins and Latz[8]. Published explicitly as a semi-flexible fiber model for dilute solutions, the authors construct a continuum model that provides a first approximation to flexibility. This is accomplished by modeling a fiber as two rods connected by a pivot allowing bead (Figure 6).

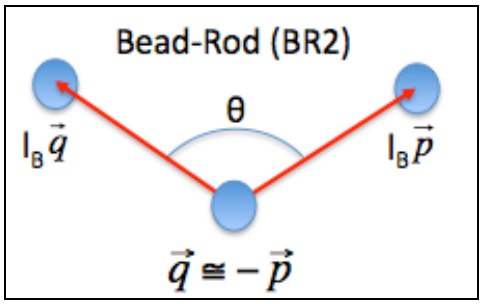

Figure 6: Fiber model, with segment length l_B, allowing semi-flexibility. The segment orientations are denoted by unit vectors $\vec{p}$ and $\vec{q}$, and are separated by an angle θ with some given bending rigidity.

The model constructs two rigid segments with length l_B that are allowed to slightly pivot about the connecting bead, with some restorative bending rigidity. Both $\vec{p}$ and $\vec{q}$ are unit vectors that represent the orientation of the corresponding fiber segments, with respect to the center bead. Restrictions, associated in the mathematical development of this model, mandate the fiber be only semi-flexible and hence $\vec{q} \cong -\vec{p}$. Additional assumptions used in this development states that the fiber has negligible inertia, inferring that the center of mass of the fiber instantaneously adjusts to changes in solvent velocity, and that the fiber is neutrally buoyant within the suspending medium. Nonetheless, the kinematics and governing Smoluchowski equation are developed for the representative fiber and used to form the following model,

$$\frac{D\underline{\underline{A}}}{Dt} = \underline{\underline{A}}\cdot\underline{\underline{\kappa}}^T + \underline{\underline{\kappa}}\cdot\underline{\underline{A}} - [(\underline{\underline{\kappa}}+\underline{\underline{\kappa}}^T):\underline{\underline{A}}]\underline{\underline{A}} + \frac{l_B}{2}[\vec{C}\vec{\mu}+\vec{\mu}\vec{C}-2(\vec{\mu}\cdot\vec{C})\underline{\underline{A}}] - 2k[\underline{\underline{B}}-\underline{\underline{A}}\,tr(\underline{\underline{B}})] \quad (7)$$

$$\frac{D\underline{\underline{B}}}{Dt} = \underline{\underline{B}}\cdot\underline{\underline{\kappa}}^T + \underline{\underline{\kappa}}\cdot\underline{\underline{B}} - [(\underline{\underline{\kappa}}+\underline{\underline{\kappa}}^T):\underline{\underline{A}}]\underline{\underline{B}} + \frac{l_B}{2}[\vec{C}\vec{\mu}+\vec{\mu}\vec{C}-2(\vec{\mu}\cdot\vec{C})\underline{\underline{B}}] - 2k[\underline{\underline{A}}-\underline{\underline{B}}\,tr(\underline{\underline{B}})] \quad (8)$$

$$\frac{D\vec{C}}{Dt} = \underline{\underline{\kappa}}\cdot\vec{C} - (\underline{\underline{A}}:\underline{\underline{\kappa}})\vec{C} + \frac{l_B}{2}[\vec{\mu}-\vec{C}(\vec{\mu}\cdot\vec{C})] - k\vec{C}[1-(tr(\underline{\underline{B}})] \quad (9)$$

$$\vec{\mu} = \sum_{i=1}^{3}\left(\sum_{j=1}^{3}\sum_{k=1}^{3}\frac{\partial^2 v_i}{\partial x_i \partial x_k}A_{jk}\right)\vec{e}_i \quad (10)$$

where the two orientation tensors represent the second moment of the distribution function of the unit vectors, $\vec{p}$ and $\vec{q}$, in the following manner:

$$\underline{\underline{A}} = \int \vec{p}\,\vec{p}\,\psi(\vec{p},\vec{q})\,d\vec{p}\,d\vec{q} \quad (11)$$

$$\underline{\underline{B}} = \int \vec{p}\,\vec{q}\;\psi(\vec{p},\vec{q})\,d\vec{p}\,d\vec{q} \quad (12)$$

As a direct consequence to the bending rigidity, encompassed within the model parameter k, the expectancy of a segment orientation (with respect to the orientation distribution function) may be non-zero in general, and is accounted in Eqn. (9) by the following definition:

$$\vec{C} = \int \vec{p}\,\psi(\vec{p},\vec{q})\,d\vec{p}\,d\vec{q} \quad (13)$$

Lastly, Eqn. (10) contributes second order derivatives of the velocity field that originate from a Taylor series approximation applied to the bead kinematics. In simple shear flow, for example, all components are *0*. This vector, in Eqn. (10), is formed by the unit dyads $\vec{e}_i$.

As with the Folgar-Tucker model, the simulation of the Bead-Rod model was given random initial orientation at the gate and analyzed at 40% of the short shot length. Similar to the simulations conducted by the model's author, the mode parameter k was set equal to a dimensionless value of *0.5*. Additionally, the segment length l_B was given a dimensionless value that approximately corresponds to 0.5 mm; however fiber attrition data may be needed for accuracy. The numerical results, and same experimental data, are given in Figure 7.

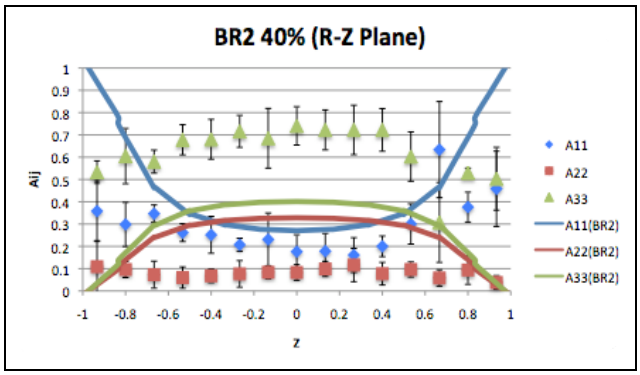

Figure 7: Bead-Rod (BR2) simulation and experimentally measured results, for the trace components of the orientation tensor, versus the dimensionless mold thickness. The components are give by "r = 1", "z = 2", "θ = 3."

The Bead-Rod simulation predicts a much broader orientation distribution, as compared to what was obtained

using the Folgar-Tucker model. Although the qualitative behavior of the orientation is better represented in this figure (especially for A_{11}), the results for A_{33} and A_{22} are different from what is observed experimentally. The simulation results with the Bead Rod model are therefore also not satisfactory in comparison with the results obtained experimentally. It should, however, be noted that the parameters available within this model should be more precisely determined, and/or fit, before full judgment of this model may be passed. This will therefore become the nature of future work.

Conclusion

In conducting the aforementioned simulations, it becomes evident that the nature of long fiber kinematics, in complex flow, is not accurately explained by either of these models and/or the assumptions used in the simulation of these models. One solution to this would be to more accurately determine and/or fit parameters for the Bead Rod model (as was done with the Folgar Tucker model) and use initially determined orientations within the simulations. This would ensure that these particular models are functioning most properly. If indeed these efforts still produce less than convincing results, the next step may be to first try understanding long fiber behavior in simple flow (rather than complex) by using well defined flows to study the desired behavior. Additionally, well-defined flows may be utilized to obtain rheological data, from which parameter data may be obtained. It is thus believed that studying long fibers in simple flow will provide a more fundamental opportunity to understand their behavior. Specifically, a sliding plate rheometer[10], that we believe is capable of conducting such studies, has been fabricated and will become the nature of further publications.

Acknowledgments

Financial of NSF/DOE: DMI-052918

References

1. A. Eberle, et al., submitted to *J. Rheol.* (2008).
2. Advani S.G. and C.L. Tucker III, *J. Rheol*. **31**, 751-84 (1987).
3. Advani S.G. and C.L. Tucker III, *J. Rheol*. **34,** 367-386 (1990).
4. D. G. Baird and D. I. Collias, *Polymer Processing*, Boston: Butterworth-Heinemann, 1998.
5. F. P. Folgar and C. L. Tucker, *J Reinf Plast Comp* **3**, 98-119 (1984).
6. Hine, P.J., Davidson, N., Duckett, R.A., *Poly. Comp.* **17**, 720–729 (1996).
7. R. S. Bay and C. L. Tucker, *Polym Eng Sci.* **32**, 240-253 (1992).
8. Strautins and Latz. *Rheol. Acta.* **46**. 1057-1064 (2007).
9. W. Smith and J. Hashemi, *Foundations of Material Science and Engineeering. McGraw Hill (2006).*
10. Xu Junke, Stéphane Costeux, *Rheo. Acta.* **46**, 815-824 (2007).
11. Velez-Garcia G.M., Ortman K.C., *ICOR Conf. Proc.* **1027**, 42-44 (2008).

Key Words: Long glass fiber orientation, injection molding, flexible fiber, composite, glass reinforced thermoplastic